Coherence Optimization and Its Limitations for Deformation Monitoring in Dynamic Agricultural Environments

Jeanine Engelbrecht and Michael R. Inggs, *Senior Member, IEEE*

***Abstract*—Differential interferometry techniques are well known for its ability to provide centimeter to millimeter scale deformation measurements. However, in natural and agricultural areas, the presence of vegetation and the evolution of the land surface introduce a phase noise component which limits successful interferometric measurement. This paper aims to address the known limitations of traditional dInSAR in the presence of disturbances to reflected signals due to agricultural activities by testing the polInSAR technique for its ability to increase interferometric coherence and to detect surface movement in the areas of interest. Both fully polarimetric RADARSAT-2 and ALOS PALSAR data were subject to coherence optimization using the multiple scattering mechanism (MSM) approach. For C-band RADARSAT-2 data, coherence optimization resulted in a statistically significant increase in interferometric coherence. However, the spatial heterogeneity of the scattering process and how it changes over time caused random phase changes associated with temporal baseline effects and the evolution of the land surface. These effects could not be removed from C-band interferograms using the MSM approach. Therefore, coherence optimization resulted in an increase in the random speckle in interferograms reducing the ability to derive high confidence interferometric measurements, indicating a drawback in the MSM approach to coherence optimization. On the other hand, coherence optimization on L-band data demonstrated an increase in the spatial homogeneity of the speckle noise suggesting that the MSM approach to coherence optimization on L-band data may be more successful in enhancing the ability to extract deformation measurements in dynamic agricultural regions. In general, a good agreement in deformation measurements derived from dInSAR and polInSAR techniques was observed.**

***Index Terms*—Coherence optimization, polInSAR, subsidence monitoring.**

I. Introduction

SURFACE deformation due to underground mining poses risks to health and safety as well as infrastructure and the environment. Consequently, the need for long-term operational monitoring systems exists. Traditional field-based measurements are point-based meaning that the full extent of deforming areas is poorly understood. Field-based techniques are also labor intensive if large areas are to be monitored on a regular basis. Radar interferometry techniques are well known for their ability to accurately detect and measure centimeter to millimeter scale surface deformation. The maturity of dInSAR has, in principle, overcome the limitations associated with field-based techniques and has been extensively used for its ability to monitor deformation over large areas, remotely. The operational limitations of dInSAR deformation measurements in commercial agricultural environments were tested using real-world deformation phenomena as test-case [1]–[4]. The results revealed that the biggest limitation of dInSAR was the presence of signal noise as a result of temporal and geometric conditions at the time of image acquisition as affirmed by others [5], [6].

Temporal decorrelation can result from a change in the position of the scatterer as well as changes in the scattering characteristics of the target. These include changes in the shape, orientation, and dielectric constant of the scatterer [6]. In a dynamic commercial agricultural region, for instance, the evolution of the land surface is quite pronounced with activities such as tilling, crop growth, and harvesting significantly altering the observed surface. These changes also affect the radar backscatter return which induces an incoherent change in the signal [7], [8]. This results in decorrelation of the signal, the severity of which depends on the wavelength and polarization of the signal. The decorrelation tends to increase with an increase in the timeframe between image acquisitions (temporal baseline) [2], [4], [9], [10]. However, decorrelation can also occur over short time periods where the random movement of leaves and twigs of vegetation implies that scattering elements are continuously rearranged, causing signal decorrelation [11]. Therefore, higher vegetation densities will be more prone to decorrelation effects and interferometric coherence will decrease rapidly with time [11]. Consequently, temporal decorrelation effects make dInSAR measurements challenging over vegetated areas [12]. In fact, dInSAR studies in agricultural environments found that, using C-band RADARSAT-2 data, very short temporal baselines would be needed for successful interferometric measurement even after the peak of the growing season when vegetation densities were lower. However, during the peak of the growing season, dInSAR measurement using even the shortest possible temporal baselines (24-days for the RADARSAT-2 data in question) was limited due to signal decorrelation by vegetation. Although longer temporal baselines could be used with longer wavelength L-band data, decorrelation of the signal due to tilling and harvesting was still evident [1], [2]. Therefore, the ability to overcome the temporal decorrelation effects, especially during

Manuscript received September 30, 2015; revised March 27, 2016 and June 26, 2016; accepted July 21, 2016. This work was supported in part by the Council for Scientific and Industrial Research and in part by the South African Council for Geoscience. *(Corresponding author: Jeanine Engelbrecht.)*

J. Engelbrecht is with the Council for Scientific and Industrial Research, Meraka Institute, Pretoria 0001, South Africa (e-mail: jengelbrecht@csir.co.za).

M. R. Inggs is with the Department of Electrical Engineering, University of Cape Town, Cape Town 7925, South Africa (e-mail: mikings@gmail.com).

Color versions of one or more of the figures in this paper are available online at http://ieeexplore.ieee.org.

Digital Object Identifier 10.1109/JSTARS.2016.2593946

TABLE I
SATELLITE DATA AND DATES OF IMAGE ACQUISITION

Data source	Acquisition date	Data source	Acquisition date
ALOS PALSAR	2008/10/27	Radarsat-2	2011/08/06
ALOS PALSAR	2009/04/29	Radarsat-2	2011/08/30
ALOS PALSAR	2009/10/30	Radarsat-2	2011/09/23
Radarsat-2	2011/01/26	Radarsat-2	2011/10/17
Radarsat-2	2011/02/19	Radarsat-2	2011/11/10
Radarsat-2	2011/03/15	Radarsat-2	2011/12/04
Radarsat-2	2011/04/08	Radarsat-2	2011/12/28
Radarsat-2	2011/05/02		

the peak of the growing season, would be needed for successful deformation measurement in agricultural environments.

The sensitivity of interferometric coherence to variations in the height and density of vegetation has been described in several investigations [13], [14]. To overcome the temporal decorrelation effects on dInSAR measurements, several advanced algorithms have been developed. These techniques rely either on the selection of pixels demonstrating ideal behavior to focus on for further processing [5], [12], [15]–[19], or the techniques are designed to directly enhance interferometric coherence [6], [14], [20]–[25]. Techniques that focus on pixels that remain coherent over the entire stack of interferograms include the persistent scatterers interferometry (PSI) and Small BAseline Subset (SBAS) techniques [5], [12]. However, in vegetated regions, the coherent or stable reflectors required when using these techniques are unavailable. To overcome this limitation, recent advances, including the SqueeSAR approach, have focused on incorporating the analysis of distributed targets in the coherent target algorithms, increasing the density of measurements in nonrural areas [19]. Alternatively, since the change in the scattering geometry that results in signal decorrelation also leads to a change in the polarimetric response in two SAR images, the introduction of SAR polarimetry into conventional interferometry has also been proposed. The combination of radar polarimetry and radar interferometry, known as polInSAR, enables the development of coherence optimization algorithms to improve the quality of interferometric measurements [13], [21]–[24], [26]. Coherence optimization is achieved by identifying the scattering mechanism that leads to the highest possible coherence and, consequently, the scattering mechanism providing the best phase estimates [21].

This paper aims to address the known limitations of traditional dInSAR in the presence of disturbances to reflected signals due to agricultural activities by testing the polInSAR technique, with the particular focus on the multiple scattering mechanism (MSM) approach to coherence optimization, for its ability to increase interferometric coherence and to detect surface movement in dynamic agricultural environments. For this purpose, 12 fully polarimetric RADARSAT-2 (Fine Quad Polarization, Beam mode FQ16) and three fully polarimetric ALOS PALSAR scenes were acquired. The dates of image acquisition are presented in Table I. This paper describes the characteristics of the study area in Section II, and Section III discusses advanced dInSAR techniques. Section IV presents the results of polInSAR coherence optimization for deformation monitoring and discusses its successes or failures. The concluding remarks and considerations for future research are provided in Section V.

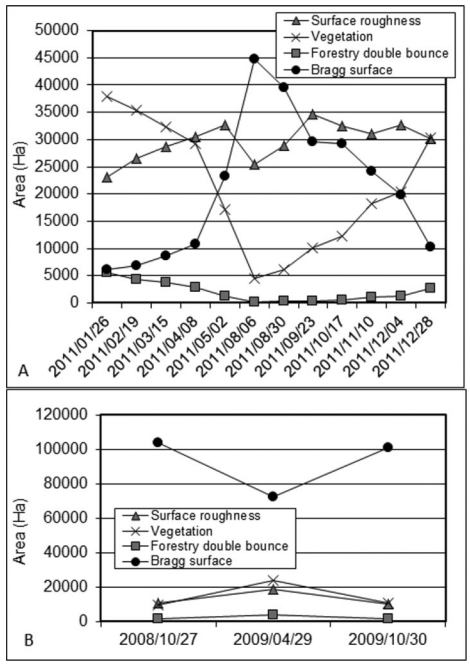

Fig. 1. (A) RADARSAT-2 H-A-alpha classification revealing the dominant scattering mechanisms over time. (B) Dominant scattering mechanisms for ALOS PALSAR data over time.

II. INTRODUCTION TO THE STUDY AREA AND PREVIOUS OBSERVATIONS

The area focused on in this investigation is situated in a coal mining region in the Mpumalanga Province of South Africa which is also subject to commercial agricultural activities [2], [4]. The exact location of the area is not disclosed due to operational sensitivity. Surface subsidence associated with near-surface coal mining in the area is a known concern and conventional dInSAR on both L-band and C-band data has been used successfully to detect and monitor surface deformations [1], [2], [4]. The surface land use is associated with commercial agricultural activity [4]. The main crop types include maize, sunflowers, and soya in addition to pasture. Planting of crops usually takes place between October and the end of November. Both soya and sunflowers ripen by the end of March, at which time the leaves of the plants disintegrate, significantly lowering the vegetation biomass. Maize is usually harvested in June except in cases where the maize is used as fodder, when harvesting can take place earlier. When maize ripens, plant leaves do not disintegrate as is the case with sunflower or soya which means that the plant retains its biomass until harvesting [4].

Previous investigations considered the limitations of conventional dInSAR approaches for deformation measurement in the area of interest using RADARSAT-2 and ALOS PALSAR data [1], [3], [4]. The dynamic agricultural nature of the area under investigation meant that temporal decorrelation effects had a

significant impact on interferometric coherence and was considered to be the biggest limitation for successful deformation measurement [2]. The temporal dynamics was further investigated by analyzing the change in the polarimetric behavior exhibited in the area over time using the H-A-alpha classification scheme [27]. For RADARSAT-2 data, volume scattering mechanisms dominated during the peak of the growing season after which surface scattering mechanisms dominated until the start of the next growing season was reached [see Fig. 1(A)]. For the periods during which surface scattering dominated, surface scattering mechanisms varied between medium entropy surface scattering and low entropy scattering. Generally, medium entropy surface scattering dominated with the exception of periods where fields were fallow during which dominance of low entropy scattering mechanisms was observed. On the other hand, the scattering mechanisms for longer wavelength PALSAR data were dominated by surface scattering mechanisms independently of the time of year [see Fig. 1(B)]. This was expected since the longer wavelength radiation penetrates through vegetation maximizing interaction with the surface. The analysis suggests that significant changes in dominant scattering mechanisms over time were observed with RADARSAT-2 data although the dominant scattering mechanisms remained constant when longer wavelength ALOS PALSAR data were considered.

III. Advanced dInSAR Approaches for Deformation Measurement

To overcome the problems associated with temporal and geometric decorrelation and atmospheric artefacts, several advanced interferometric processes have been developed [5], [12], [15], [16], [18]. Techniques that focus on pixels that remain coherent over the entire stack of interferograms include the PSI and SBAS techniques [5], [12]. The coherent pixels are stable natural reflectors usually corresponding to man-made structures or rock-outcrops [12], [28] meaning that in vegetated, nonurban areas, the density of coherent pixels may be very low limiting the viability of the SBAS and PSI techniques in these areas [6], [17]. To increase the quality of measurements in nonurban areas, recent advances, including the distributed scatterers interferometry [29] and the SqueeSAR approach [19], [30], have focused on including the analysis of distributed targets. The joint processing of distributed and coherent targets, as implemented in the SqueeSAR algorithm [19], results in a significant increase in the density and quality of measurement points in nonurban regions [19], [31]. However, the distributed targets are associated with statistically homogeneous pixels and are generally associated with debris areas, noncultivated land with very sparse vegetation and desert areas [19], [30], suggesting limited applicability in agricultural fields.

As an alternative to the analysis of pixels demonstrating ideal behavior, techniques to directly enhance coherence have also been proposed. Temporal decorrelation not only has an effect on the interferometric coherence, but also leads to different polarimetric responses in two SAR images [10], [20]. Therefore, the introduction of polarimetry into conventional interferometry has been proposed [32]. These advanced dInSAR techniques have focused on exploiting the polarimetric properties of SAR signals to maximize interferometric coherence as opposed to merely selecting the high coherence targets for further processing [10], [22]. The sensitivity of backscatter in different polarizations to the shape, orientation, and dielectric properties of the scattering elements allows for the identification and separation of scattering mechanisms by investigating the differences in polarimetric signatures [14]. Several coherent and incoherent scattering target decomposition theorems have been developed with the objective to extract information about scattering behavior from volumes and surfaces [27] allowing the description of ground/volume scattering scenarios [25]. These target decomposition theorems have also been introduced in interferometry to advance the interpretation of interferometric phase in an effort to minimize temporal decorrelation effects [6], [13], [14], [20]–[23], [33], [34].

The ability to identify and separate scattering mechanisms from polarimetric signatures implies that the combination of interferometric and polarimetric information can be used to infer the interferometric phase of any scattering mechanism and, consequently, the vertical distribution of different scattering mechanisms [14], [21], [34]. The combination of radar polarimetry and radar interferometry is known as polarimetric interferometry (polInSAR) and the mathematical formulation can be obtained in various published works [14], [27], [34], [35].

PolInSAR allows for the retrieval of the height of different scattering mechanisms present in a resolution cell, even if one scattering mechanisms dominates over another [25]. Consequently, polInSAR also enables the development of coherence optimization algorithms to improve the quality of interferometric measurements [13], [20]–[24], [26], [33]. This is achieved by identifying the scattering mechanism which leads to the highest possible coherence and, consequently, the scattering mechanism providing the best phase estimates [21]. Different approaches are taken to select the optimal scattering mechanism including the MSM approach and the equal scattering mechanism (ESM) approach [21].

The ESM optimization process involves the simultaneous search for the optimized coherence and the corresponding scattering mechanism [23] with the constraint that ESMs are selected [6], [23], [33]. The ESM approach ensures the selection of equal polarimetric signatures on a pixel-by-pixel basis representing the overall dominant scattering mechanism [6], [23], [33]. The drawback of the ESM approach is that it assumes that the polarimetric behavior across datasets do not change [23] which implies that small temporal and perpendicular baseline datasets are needed [33]. In cases where a large amount of temporal decorrelation exists, the polarimetric behavior of surfaces can change significantly, leading to an insufficient number of scatterers exhibiting the same behavior. This can limit the effectiveness of this approach [33], [36]. Therefore, the ESM approach is constrained to areas that do not undergo significant changes in the polarimetric behavior over time.

In the case of strong temporal dynamics of an area under investigation, the MSM approach has been recommended as the preferred approach to coherence optimization [23]. Since significant changes in the polarimetric behavior of the area of interest

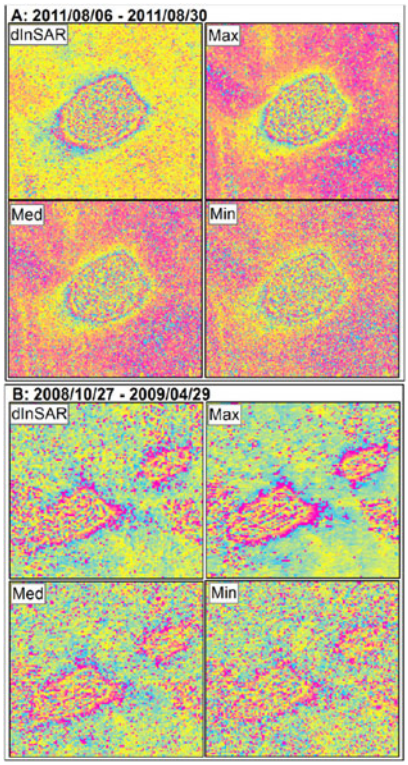

Fig. 2. Comparison of dInSAR interferogram and coherence optimized interferograms for (A) the 2011/08/06–2011/08/30 RADARSAT-2 interferometric pairs and (B) 2008/10/27–2009/04/29 ALOS PALSAR data.

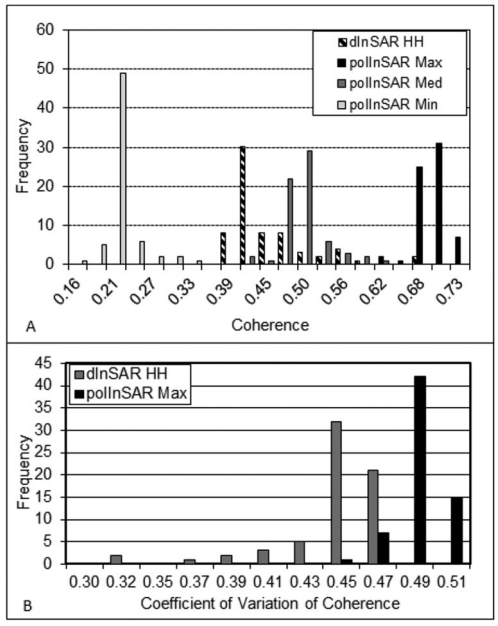

Fig. 3. (A) Frequency distribution of average scene coherence values for dInSAR (HH) processing and the maximum (polInSAR max), minimum (polInSAR min), and intermediate (polInSAR med) results. (B) CV of coherence values for polInSAR and dInSAR results.

[see Section II and Fig. 1(A)] as well as temporal decorrelation effects (Section II, [4]) are present due to the agricultural nature of the area of interest, the MSM optimization was considered in this investigation. In contrast to the ESM approach, the MSM approach relies on the identification of the scattering mechanisms that provide the highest possible coherence, with the assumption that the scattering mechanism that provides the highest possible interferometric coherence can vary between neighboring pixels. Therefore, different scattering mechanisms can contribute to the optimal phase [6], [23], [24], [33].

The MSM approach to coherence optimization was performed on both RADARSAT-2 and ALOS PALSAR fully polarimetric data. The resulting interferometric coherence and deformation data were compared to the results obtained by conventional dInSAR techniques (presented in Section IV) to determine the success or limitations of these approaches for long-term deformation measurement strategies (presented in Section V).

IV. Data Processing and Coherence Optimization Results

To assess the ability of coherence optimization algorithms to increase interferometric coherence in the agricultural area of interest, the MSM technique for coherence optimization was used. The selection of the MSM technique was governed by the fact that polarimetric analysis of the RADARSAT-2 data revealed that the dominant scattering mechanisms are highly variable over time [4] (see Section II). The result of the coherence optimization algorithm is three interferograms, representing high, medium, and low coherence products. The interferograms were constructed by identifying the dominant scattering mechanisms and separating those representing the highest coherence values from the scattering mechanisms exhibiting intermediate and low coherence values. By selecting only the scattering mechanisms leading to the highest possible coherence, the best phase estimates are obtained. The interferograms generated for the RADARSAT-2 2011/08/06–2011/08/30 interferometric pair are displayed in Fig. 2(A) where the dInSAR interferogram is displayed alongside the max (maximum coherence), med (intermediate coherence), and min (minimum coherence) interferograms generated by polInSAR. Similarly, the ALOS PALSAR interferograms generated between 2008/10/27 and 2009/04/29 are displayed in Fig. 2(B). Visual inspection of the resulting interferograms suggests that noisy areas in interferograms generated by dInSAR remain noisy on the interferograms generated by coherence optimization using polInSAR techniques.

To further explore this observation, the interferometric coherence calculated by conventional dInSAR techniques was compared to the interferometric coherence generated by the polInSAR techniques. The frequency distribution of the average scene coherence for dInSAR and polInSAR coherence is presented in Fig. 3(A) for RADARSAT-2 data. For all datasets, the maximum coherence values obtained by coherence optimization techniques are significantly higher than the coherence values obtained through conventional dInSAR. However, interferometric measurement on a single pixel is not sensible since single pixels can incorporate phase noise in an unpredictable way. The random nature of the phase noise in interferograms was estimated by calculating the coefficient of variation (CV) of

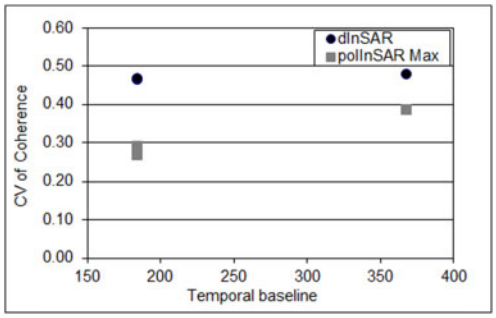

Fig. 4. CV of coherence values for ALOS PALSAR polInSAR and dInSAR results.

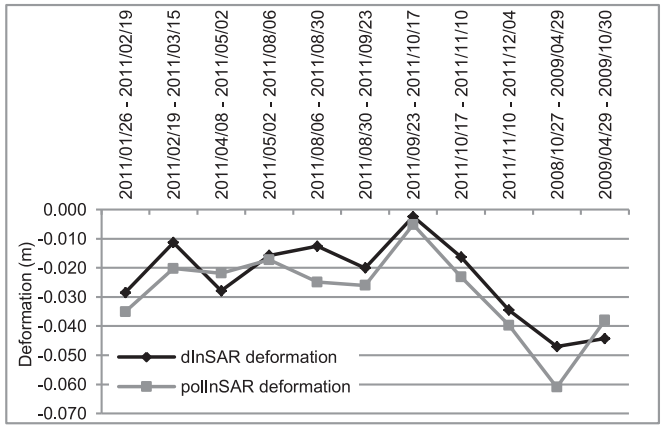

Fig. 5. Comparison of dInSAR and polInSAR deformation measurements.

the coherence values for each pixel considering a neighborhood of 11 by 11 pixels. Lower CV values indicate more homogenous neighborhoods (lower variance) while higher CV values indicate more heterogeneous data. The CV of coherence values was calculated for RADARSAT-2 data for the conventional dInSAR coherence and the maximum coherence result of the coherence optimization algorithm [see Fig. 3(B)]. The results indicate that a consistently higher CV of coherence is achieved after coherence optimization compared to a lower CV without coherence optimization for RADARSAT-2 data. This suggests that although polInSAR leads to a statistically significant increase in the average coherence, the effect of random phase changes is not minimized.

Since only three fully polarimeric ALOS PALSAR scenes were available for analysis, statistical interpretation of coherence optimization results is not possible. However, for the PALSAR data, a significant decrease in CV of coherence is observed for the coherence optimized data compared to conventional dInSAR coherence data (see Fig. 4). This suggests that polInSAR coherence optimization on L-band data may provide both an increase in the interferometric coherence and the decrease in the random phase changes between neighboring pixels that is required for high confidence interferometric measurement.

To compare the deformation measurements achieved for dInSAR and polInSAR approaches, the average deformation measurements were extracted for each of the deformation features observed. The average measured vertical deformation for dInSAR and polInSAR results is displayed, graphically, in Fig. 5. Unfortunately, a lack of *in situ* measurements for the observation period means that an assessment of whether dInSAR or polInSAR results were more accurate could not be made. However, the differences between polInSAR and dInSAR deformation measurements are low (less than 7 mm with three exceptions). In general, dInSAR deformation maps reflect lower vertical displacements compared to the polInSAR deformation maps. For RADARSAT-2 data, an exception is observed for the 2011/04/08–2011/05/02 interferograms for which the measured dInSAR subsidence is higher than polInSAR measurement. It should be noted that the period between 2011/04/08 and 2011/05/02 is associated with an increase in surface scattering contributions and concurrent decrease in vegetation scattering contribution [see Fig. 1(A) and Section II].

The apparent increase in measured deformation for dInSAR deformation maps may be indicative of a higher phase center on the stems of the vegetation on the 2011/04/08 scene followed by a lower phase center on the 2011/05/02 scene where surface scatterers dominate. The shift in phase center depending on the height of the dominant scattering mechanism therefore results in an artificial increase in the measured deformation in dInSAR results. Since the measured deformation is lower on polInSAR deformation maps, it is assumed that the change in phase center does not affect polInSAR deformation maps to the same degree. It is also observed that the difference between polInSAR and dInSAR deformation measurements is smaller for the periods during which surface scattering mechanisms dominate (between 2011/05/02 and 2011/11/10). An exception is observed for the 2011/08/06–2011/08/30 interferometric pair which reflects a difference of 1.2 cm between polInSAR and dInSAR deformation measurements. This period is associated with predominantly smooth (low entropy) surface scattering mechanisms. Therefore, a higher degree of similarity between dInSAR and polInSAR deformation measurements would be expected. The large difference is considered to be anomalous and warrants further investigation.

For ALOS PALSAR results, dInSAR reflects a larger amount of subsidence for the 2009/04/29–2009/10/30 pair compared to polInSAR subsidence measurements. Although this time period is also associated with a decrease in vegetation scattering [see Fig. 1(B) and Section II], smooth surface scattering mechanisms dominate on both acquisition dates for the long wavelength data. Therefore, a decrease in scattering phase center between 2009/04/29 and 2009/10/30 would not be expected. However, the difference between polInSAR and dInSAR measurements (6 mm) is considered to be small. On the other hand, the difference between the polInSAR and dInSAR deformation measurements for the 2008/10/27–2009/04/29 pair is 1.4 cm. The period is associated with an increase in volume scattering mechanisms, although low entropy surface scattering remains dominant on both acquisitions. Therefore, the height difference between scattering centers would not be expected although it could explain the perceived decrease in the amount of vertical displacement exhibited by dInSAR compared to polInSAR deformation maps.

V. Discussion and Considerations for Future Research

In this study, coherence optimization was tested for its ability to increase interferometric coherence in an agricultural area. The results suggest that although a statistically significant increase in the average scene coherence was achieved, the CV for polInSAR results on C-band data was consistently higher than the CV for dInSAR results. This indicates a decrease in the spatial homogeneity of the phase noise contribution leading to an increase in speckle noise effects. This decrease in the homogeneity of the phase noise also translated to the interferometric phase, leading to increased speckle effects and decreasing the ability to derive high confidence interferometric measurements. In general, noisy areas in interferograms generated through dInSAR techniques remain noisy on the interferograms generated through polInSAR techniques. The results suggest that although coherence optimization techniques results in a statistically significant increase in coherence, especially in the maximum coherence results, the apparent decrease in phase noise is not translated to the interferograms generated using the coherence optimization technique. Despite the apparent increase in the phase heterogeneity by polInSAR algorithms, there is a good agreement between the measured vertical deformations derived from dInSAR compared to polInSAR techniques with a mean difference of 6.2 mm observed. Furthermore, for a period associated with a change in dominant scattering mechanism from vegetation scattering to surface scattering, dInSAR results may be affected by an overestimation of vertical displacement induced by a change in the height of the scattering phase center (i.e., a higher phase center experienced where volume scattering dominated compared to where surface scattering dominates). The effect appears to be minimized when polInSAR results are considered. Although the number of datasets is insufficient, the results suggest that for periods coinciding with a change in dominant scattering mechanism from volume to surface scattering or vice versa, polInSAR techniques can lead to higher accuracy deformation measurements.

Where phase noise is concerned, an explanation for the failure of coherence optimization techniques in minimizing the phase noise component is the dominant scattering processes in the scene and how they change between master and slave image acquisitions. Although polarimetric analysis proved that the dominant scattering mechanism for the 2011/08/06 and 2011/08/30 scenes is low entropy surface scattering (see Section II), some volume scattering contributions and surface roughness propagation effects were also observed. Post-classification change detection algorithms on the H-A-alpha classification results were used to highlight the dominant changes in scattering mechanisms between image acquisitions.

An example of the changes in scattering mechanism between master and slave image acquisition is presented in Fig. 6 using a subset of the 2011/08/06–2011/08/30 pair as example. The results for this pair show that significant changes in the dominant scattering mechanism over time is experienced with Bragg surface scattering changing to surface roughness propagation effects being the most dominant change. Surface roughness propagation effects changing to volume scattering (vegetation) are also observed. The observed changes in scattering mechanism

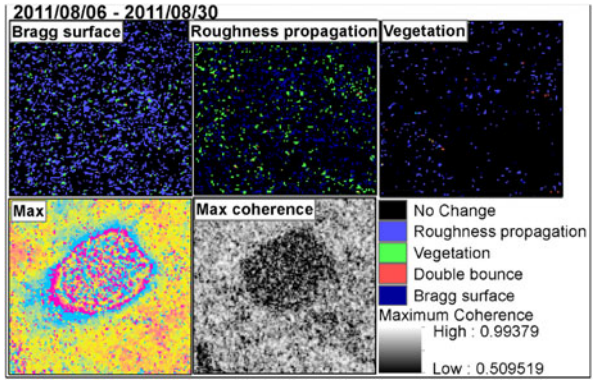

Fig. 6. Scattering mechanism changes between 2011/08/06 and 2011/08/30 for RADARSAT-2 data. The top row labeling indicates the initial scattering state on 2011/08/06 as Bragg surface scattering, roughness propagation effects and vegetation, respectively. The colors indicate the scattering mechanism change reflected on 2011/08/30.

were spatially heterogeneous and, together with the volume scattering contributions, introduce random phase changes between the master and slave image acquisitions which cannot be removed by polInSAR techniques. Additionally, when the maximum coherence image (see Fig. 6) is considered, it is apparent that the subsiding area is associated with low interferometric coherence. The low coherence is due to the deformation between 2011/08/06 and 2011/08/30 exceeding the 2.8 cm per pixel gradient limit imposed by the wavelength of the RADARSAT-2 sensor. This implies that even if the phase contribution from surface scattering mechanisms could be isolated to provide very high coherence interferograms, surface deformation exceeding the gradient limit would continue to cause incoherence and polInSAR is not capable of minimizing the phase noise in these areas.

Although the L-band data are associated with an enhanced ability to penetrate through vegetation and is predominantly associated with surface scattering contributions (see Section II), post classification change detection on the classification based on scattering mechanism reveals that changes in scattering mechanisms between master and slave image acquisitions are still taking place, although to a lesser extent than was observed for C-band data. In this case, a higher likelihood of selecting the same scattering mechanism over time may have contributed to a decrease in the CV of coherence and higher confidence interferometric measurements on L-band data. Despite the increase in phase heterogeneity and the lower sensitivity of PALSAR data to a change in vegetation cover, the mean difference between the dInSAR and polInSAR deformation measurements was greater than observed for RADARSAT-2 scenes with a mean difference of 1.0 cm observed. However, the number of quad-pol ALOS PALSAR scenes available for analysis was insufficient to draw accurate conclusions.

The drawback of the MSM technique for differential applications on C-band data is that the scattering mechanism that provides the highest possible interferometric coherence can vary between neighboring pixels and different scattering mechanisms can contribute to the optimal phase [6], [23], [24]. In fact, it was observed that in a multibaseline approach to the MSM optimization, varying polarizations in different datasets will have

to be taken into account [23], [33]. Since different scattering mechanisms will provide phase measurements at different phase centers, topographic phase will be incorporated depending on the scattering mechanism that provides the best coherence [22]. In this investigation, different scattering mechanisms over time provided phase measurements at different phase centers, introducing an element of heterogeneity into interferograms derived from C-band data. On the other hand, coherence optimization on L-band data demonstrated an increase in the spatial homogeneity of the coherence after optimization algorithms were applied. This suggests that the coherence optimization algorithms were more likely to select the same scattering mechanism between neighboring pixels that would lead to more homogeneous results. Therefore, although the number of fully polarimetric L-band interferometric pairs was insufficient to be conclusive, the results suggest that coherence optimization may be more successful in minimizing phase noise on longer wavelength data in dynamic agricultural environments. Future activities will focus on increasing the number of L-band datasets for more in-depth analysis.

Since the study area in question was shown to exhibit strong temporal dynamics, the assumption was that the MSM approach would be successful to optimize coherence and enhance our ability to measure surface deformation in a dynamic agricultural region. However, the results demonstrated that the heterogeneity introduced by selecting different scattering mechanisms in the MSM approach meant that phase noise could not be entirely eliminated. Therefore, although the polarimetric behavior of the dataset in question is not constant as is assumed when implementing the ESM algorithm, the ESM approach will be tested for its ability to reduce the spatial heterogeneity of the phase measurements in future research. Since the ESM approach involves coherence optimization with the constraint that ESMs are selected (see Section III), it is believed that the ESM approach will ensure the selection of equal polarimetric signatures, thereby increasing intereferometric coherence and decreasing the random phase changes leading to higher confidence interferometric measurement. It is also recommended that future research exploits advanced algorithms, such as the CEASAR algorithm [31], which is similar to SqueeSAR with the exception that temporal and baseline decorrelation effects are counteracted by selecting the dominant scattering mechanism in an interferometric stacking approach [31].

REFERENCES

[1] J. Engelbrecht and M. Inggs, "Recommendations for long-term operational dinsar monitoring of mining-induced deformation in a dynamic agricultural region," in *Proc. Int. Geosci. Remote Sens. Symp.*, 2013, pp. 2912–2915.

[2] J. Engelbrecht, *Parameters Affecting Interferometric Coherence and Implications for long-Term Operational Monitoring of Mining-Induced Deformation*. Cape Town, South Africa: Univ. Cape Town, 2013.

[3] J. Engelbrecht and M. Inggs, "Differential interferometry techniques on L-band data employed for the monitoring of surface subsidence due to mining," *South African J. Geomatics*, vol. 2, no. 2, pp. 82–93, 2013.

[4] J. Engelbrecht, C. Musekiwa, J. Kemp, and M. R. Inggs, "Parameters affecting interferometric coherence—The case of a dynamic agricultural region," *IEEE Trans. Geosci. Remote Sens.*, vol. 52, no. 3, pp. 1572–1582, Mar. 2014.

[5] C. Prati, A. Ferretti, and D. Perissin, "Recent advances on surface ground deformation measurement by means of repeated space-borne SAR observations," *J. Geodyn.*, vol. 49, nos. 3/4, pp. 161–170, 2010.

[6] A. Reigber, M. Neumann, E. Erten, M. Jäger, and P. Prats, "Multi-baseline polarimetrically optimised phases and scattering mechanisms for InSAR applications," in *Proc. IEEE Int. Geosci. Remote Sens. Symp.*, 2007, no. 4, pp. 2620–2623.

[7] X. Blaes and P. Defourny, "Retrieving crop parameters based on tandem ERS 1/2 interferometric coherence images," *Remote Sens. Environ.*, vol. 88, no. 4, pp. 374–385, 2003.

[8] D. Massonnet and K. L. Feigl, "Radar interferometry and its application to changes in the Earth's surface," *Rev. Geophys.*, vol. 36, no. 4, p. 441–500, 1998.

[9] C. Carnec and C. Delacourt, "Three years of mining subsidence monitored by SAR interferometry, near Gardanne, France," *J. Appl. Geophys.*, vol. 43, no. 1, pp. 43–54, 2000.

[10] Z. Perski and D. Jura, "Identification and measurement of mining subsidence with SAR interferometry: Potentials and limitations," in *Proc. 11th FIG Symp. Deformation Meas.*, Santorini, Greece, 2003, pp. 1–7.

[11] W. Grey and A. Luckman, "Deriving urban topography from multibaseline SAR interferometric phase coherence images," *Eur. Space Agency*, no. 461, pp. 1664–1672, 2000.

[12] A. Ferretti, C. Prati, and F. Rocca, "Permanent scatters in SAR interferometry," *IEEE Trans. Geosci. Remote Sens.*, vol. 39, no. 1, pp. 8–20, Jan. 2001.

[13] S. R. Cloude and K. P. Papathanassiou, "Coherence optimisation in polarimetric SAR interferometry," in *Proc. IEEE Int. Geosci. Remote Sens. Symp.*, 1997, pp. 1932–1934.

[14] K. P. Papathanassiou and S. R. Cloude, "Single-baseline polarimetric SAR interferometry," *IEEE Trans. Geosci. Remote Sens.*, vol. 39, no. 11, pp. 2352–2363, Nov. 2001.

[15] P. Berardino, G. Fornaro, R. Lanari, and E. Sansosti, "A new algorithm for surface deformation monitoring based on small baseline differential SAR interferograms," *IEEE Trans. Geosci. Remote Sens.*, vol. 40, no. 11, pp. 2375–2383, Nov. 2002.

[16] L. D. Euillades, P. A. Euillades, A. Pepe, M. H. Blanco, and J. H. Barón, "On the generation of late ERS deformation time series through small Doppler and baseline subsets differential SAR interferograms," *IEEE Geosci. Remote Sens. Lett.*, vol. 8, no. 2, pp. 238–242, Mar. 2011.

[17] D. L. Galloway and J. Hoffmann, "The application of satellite differential SAR interferometry-derived ground displacements in hydrogeology," *Hydrogeol. J.*, vol. 15, no. 1, pp. 133–154, 2007.

[18] O. Mora, J. J. Mallorqui, and A. Broquetas, "Linear and nonlinear terrain deformation maps from a reduced set of interferometric SAR images," *IEEE Trans. Geosci. Remote Sens.*, vol. 41, no. 10, pp. 2243–2253, Oct. 2003.

[19] A. Ferretti, A. Fumagalli, F. Novali, C. Prati, F. Rocca, and A. Rucci, "A new algorithm for processing interferometric data-stacks: SqueeSAR," *IEEE Trans. Geosci. Remote Sens.*, vol. 49, no. 9, pp. 3460–3470, Sep. 2011.

[20] S. R. Cloude and K. P. Papathanassiou, "Polarimetric SAR interferometry," *IEEE Trans. Geosci. Remote Sens.*, vol. 36, no. 5, pp. 1551–1565, Sep. 1998.

[21] E. Colin, C. Titin-Schnaider, and W. Tabbara, "An interferometric coherence optimization method in radar polarimetry for high-resolution imagery," *IEEE Trans. Geosci. Remote Sens.*, vol. 44, no. 1, pp. 167–175, Jan. 2006.

[22] V. D. Navarro-Sanchez, J. M. Lopez-Sanchez, and F. Vicente-Guijalba, "A contribution of polarimetry to satellite differential SAR interferometry: Increasing the number of pixel candidates," *IEEE Geosci. Remote Sens. Lett.*, vol. 7, no. 2, pp. 276–280, Apr. 2010.

[23] M. Neumann, L. Ferro-Famil, and A. Reigber, "Multibaseline POLinSAR coherence modelling and optimization," in *Proc. Int. Geosci. Remote Sens. Symp.*, 2007, pp. 2624–2627.

[24] L. Pipia, X. Fabregas, A. Aguasca, C. Lopez-Martinez, and J. J. Mallorquí, "Polarimetric coherence optimization for interferometric differential applications," in *Proc. Int. Geosci. Remote Sens. Symp.*, vol. 5, 2009, pp. 146–149.

[25] L. Sagués, J. M. Lopez-Sanchez, J. Fortuny, X. Fabregas, A. Broquetas, and A. J. Sieber, "Polarimetric radar interferometry for improved mine detection and surface clutter rejection," *IEEE Trans. Geosci. Remote Sens.*, vol. 39, no. 6, pp. 1271–1278, Jun. 2001.

[26] C. Lopez-Martinez, X. Fabregas, and L. Pipia, "PolSAR and PolInSAR model based information estimation," in *Proc. IEEE Int. Geosci. Remote Sens. Symp.*, 2009, pp. III-959–III-962.

[27] S. R. Cloude and E. Pottier, "An entropy based classification scheme for land applications of polarimetric SAR," *IEEE Trans. Geosci. Remote Sens.*, vol. 35, no. 1, pp. 68–78, Jan. 1997.
[28] D. Raucoules, C. Colesanti, and C. Carnec, "Use of SAR interferometry for detecting and assessing ground subsidence," *Comptes Rendus Geosci*., vol. 339, no. 5, pp. 289–302, 2007.
[29] K. Goel and N. Adam, "A distributed scatterer interferometry approach for precision monitoring of known surface deformation phenomena," *IEEE Trans. Geosci. Remote Sens.*, vol. 52, no. 9, pp. 5454–5468, Sep. 2014.
[30] J. Morgan, G. Falorni, A. Bohane, and F. Novali, *Advanced InSAR Technology (SqueeSARTM) for Monitoring Movement of Landslides*. Lakewood, CO, USA: Central Federal Lands Highway Division, 2011.
[31] G. Fornaro, S. Verde, D. Reale, and A. Pauciullo, "CAESAR: An approach based on covariance matrix decomposition to improve multibaseline–multitemporal interferometric SAR processing," *IEEE Trans. Geosci. Remote Sens.*, vol. 53, no. 4, pp. 2050–2065, Apr. 2015.
[32] O. Stebler, E. Meier, and D. Nüesch, "Multi-baseline polarimetric SAR interferometry—First experimental spaceborne and airborne results," *ISPRS J. Photogrammetry Remote Sens.*, vol. 56, no. 3, pp. 149–166, 2002.
[33] M. Neumann, L. Ferro-Famil, and A. Reigber, "Multibaseline polarimetric SAR interferometry coherence optimization," *IEEE Geosci. Remote Sens. Lett.*, vol. 5, no. 1, pp. 93–97, Jan. 2008.
[34] K. P. Papathanassiou and S. R. Cloude, "Polarimetric effects in repeat-pass SAR interferometry," in *Proc. IEEE Int. Geosci. Remote Sens. Symp.*, vol. 4, 1997, pp. 1926–1928.
[35] W. M. Boerner and J. S. Verdi, "Advances in polarimetric SAR interferometry and its application to geo/eco-environmental stress change monitoring," in *Proc. 12th Int. Conf. Microw. Radar*, 1998, pp. 277–303.
[36] Z. Binghuang and C. Bing, "An analysis of coherence optimization methods in PolInSAR," in *Proc. 1st Asian Pacific Conf. Synthetic Aperture Radar*, 2007, pp. 577–579.

Jeanine Engelbrecht received the B.Sc. (hons.) degree in geology 2003 and the M.Sc. degree in geographic information systems 2005 from the University of Stellenbosch, Stellenbosch, South Africa, and the Ph.D. degree through the Department of Electrical Engineering, University of Cape Town, Cape Town, South Africa.

She is a Principal Researcher at the Council for Scientific and Industrial Research, Meraka Institute, Pretoria, South Africa. Her research interests include remote sensing for geological investigations with a particular focus on deformation hazard assessment and monitoring.

Michael R. Inggs (SM'11) was born and educated in the Eastern Cape, South Africa (Uitenhage and Grahamstown). He received the Honors degree in physics and applied mathematics from Rhodes University, Grahamstown, in 1973, and the Ph.D. degree and DIC in Electrical and Electronics Engineering from Imperial College London, London, U.K., in 1979.

He has worked in industry in the U.K., USA, and South Africa, and joined the Department of Electrical Engineering, University of Cape Town (UCT), Cape Town, South Africa, in 1988, where he is a Professor. He held a Visiting Professorship in University College London, and was a visiting Professor at TU Delft in 2015. His research is in the area of radar, radar remote sensing, and high performance computing. He has more than 200 journal and conference publications, four patents, and has supervised more than 100 M.Sc. and 18 Ph.D. to completion.

Dr. Inggs is a member of the Administration Committee of the IEEE Geoscience and Remote Sensing Society 2011–2016 as the Director of Education, a member of IEEE Aerospace and Electronic Systems Society (AESS) Radar Panel, and was the Convenor of the taught masters M.Eng. (radar) programme at UCT from inception in 2011 to 2015. In 2015, a paper in the IEEE AESS Magazine won the Harry Mimno award for the UCT team.